Int. J. Electrochem. Sci., 14 **(2019)** 3024 – 3034, doi: 10.20964/2019.03.27

International Journal of
ELECTROCHEMICAL
SCIENCE
www.electrochemsci.org

Synthesis Metal-free Nitrogen-doped Porous Carbon by Removing Al from Al-MOFs as an Efficient Electrocatalyst for Oxygen Reduction Reaction

Yan Zhang[1,†], *Yu Zhou*[1,†], *Zonghua Wang*[*,1], *Shenlong Zhao*[2], *Chunhui Tan*[3] *and Jishi Chen*[1]

[1] Shandong Sino-Japanese Center for Collaborative Research of Carbon Nanomaterials, College of Chemistry and Chemical Engineering, Qingdao University, Qingdao 266071, China.
[2] UNSW-CWRU International Joint Laboratory, School of Chemical Engineering, the University of New South Wales, Sydney, NSW 2052, Australia.
[3] Key Laboratory for Biomass Gasification Technology of Shandong Province, Energy Research Institute, Qilu University of Technology (Shandong Academy of Sciences), Jinan, 250014, China
† These authors contributed equally to this work
[*]E-mail: wangzonghua@qdu.edu.cn

Received: 27 October 2018 / *Accepted:* 17 December 2018 / *Published:* 7 February 2019

Exploring cheap and stable electrocatalyst for the oxygen reduction reaction (ORR) is now an important issue for the large-scale application of fuel cells. Herein, we have demonstrated a facile synthesis of Nitrogen-doped porous carbons (NPC-MILs) for oxygen reduction reaction by using an amine functionalized Al-MOFs (NH_2-MIL-53(Al)) as the precursor with both nitrogen source and carbon source. NPC-MILs as metal-free electrocatalysts are demonstrated promising potential for ORR. The optimized NPC-MIL-900 (carbonized at 900 °C) exhibits a likeness four-electron process and its ORR catalytic activity can be comparable to commercial Pt/C. Furthermore, chronoamperometric measurement shows that only 13% loss at the current density is occurred after 40000 s, whereas the corresponding current density loss at the Pt/C (20wt%) is as high as 31%. Chronoamperometric responses also show the NPC-MIL-900 catalyst has higher resistance to methanol in alkaline electrolyte than Pt/C. Those indicate that the NPC-MIL-900 has potential application in fuel cells.

Keywords: electrocatalyst, metal-free, oxygen reduction reaction, N-doped microporous carbon material, metal-organic framework

1. INTRODUCTION

With depleting fossil fuels and growing environmental issues, the development of sustainable and environmental-friendly energy conversion technologies with high efficiency is urgent. Fuel cells and

metal-air batteries, as two high efficiency energy conversion, have attracted much more concerns.[1-3] Unfortunately, the sluggish cathodic electrode involving in oxygen reduction reaction (ORR) seriously impeded the output power density of these devices.[4-6] Although metal based materials, especially for platinum and Pt-based catalysts possess the good activities for ORR, it is impossible to apply them in large-scale commercial applications due to their high costs, poor durabilities, fuel crossover, and CO poisoning effects.[7-10] Therefore, it is highly desirable to develop alternative non-noble metal electrocatalysts with low cost and high efficiency.[11]

Metal-free porous carbons electrocatalysts possess several notable advantages, as they do not suffer from CO poisoning fuel or crossover effect, have high stability, and are relatively cost-effective. Metal-organic frameworks (MOFs) as hot porous, possess many unique merits, for example, ordered three-dimensional framework structures, large accessible surface areas,[12,13] which gives a great chance to make these materials as precursors or self-sacrificial templates of ORR electrocatalysts.[14-19] Now the investigations mainly focus on transition metal (for example, Fe, Co, Ni and Mn)-organic frameworks,[20-24] Indeed, MOFs are also an ideal platform for designing high performance carbon based metal-free catalysts: First, the metals (for example, Zn or Al) with low melting point can be completely removed during the high temperature pyrolysis process, meanwhile, the carbon frameworks including high surface area and pore structure still can be maintained. Second, the charge density of the carbon can be effectively adjusted by introducing different dopants through changing the groups on the ligands, which is key for improving the ORR activity. Third, carbon-based metal-free materials are robust in various electrolytes including alkalinity and acidity, which has an advantage for the durability of the catalysts.[11,25]

MOFs possess special superiority to prepare porous carbon materials. Carbonized MOFs as metal-free Nitrogen-doped porous carbons (NPC) has been investigated by utilizing Zn-based MOFs as the precursors.[11] Al-MOFs as the precursor are seldom reported. In the carbonization process, the Al ions could be reduced to Al metals (melting point 660 ^{o}C), and then removed. The residual was further leached out by the following acidification. Inspired by above, in this work, an amine functionalized Al-MOFs (NH_2-MIL-53(Al)) was used as the precursor with both nitrogen source and carbon source. At high temperature, Al in NH_2-MIL-53(Al) can be removed to become metal-free NPC catalysts. Because the high surface area, high ratio of the micropores and uniform pore size can be well inherited, the obtained NPC catalysts exhibited great onset potential (0.82 V) and half-wave potential (0.76 V), which is compared to those (0.96 V and 0.85 V) of the commercial Pt/C. Furthermore, the prepared catalysts possess the superior stability and methanol tolerance than that of commercial Pt/C in alkaline electrolyte, exhibiting a promising application in practical direct methanol fuel cells.

2. EXPERIMENTAL SECTION

2.1 Reagent and materials

Nafion solution (5%), Platinum on graphitized carbon (Pt/C, 20wt%), and aluminium nitrate nonahydrate (≥98%) were obtained from Sigma-Aldrich. 2-Amion-1,4-benzenedicarboxylic acid (NH_2-

BDC), Aluminium (III) chloride hexahydrate ($AlCl_3 \cdot 6H_2O$), and *N*,*N*-dimethylformamide (DMF) were purchased from Aladdin. Dimethyl ketone was obtained from Shanghai Chemical Reagent Inc. All chemicals were used without further purification.

2.2 Synthesis of NH_2-MIL-53 (Al) crystals

The NH_2-MIL-53(Al) crystals were synthesized by a hydrothermal method according to the previous report.[26] In a typical synthesis, NH_2-BDC (0.76 g), $AlCl_3 \cdot 6H_2O$ (0.56 g) were dissolved in 2 mL and 2 mL of DMF-H_2O mixed solvent systems, respectively. The volume ratio of water and DMF, we chosen, was 1:0.5, 1:1, 1:2, 1:3, 1:4, respectively. Subsequently, the two separate solutions were mixed together rapidly. Then, the mixture was decanted into Teflon-lined steel autoclave and kept heating at 150 °C for 24 hours in an oven. After cooling and centrifugation, the light yellow products were obtained.All the samples were activated in boiling DMF for 5 hours to remove the remaining water and unreacted ligands trapped. Finally, all the products were separated by centrifugation and washed with dimethyl ketone. The products were dried for 12 hours in a vacuum oven at 30 °C.

2.3 Synthesis of microporous carbon NPC-MIL-n

The as-prepared MOFs (NH_2-MIL-53(Al)) were pyrolyzed to carbon samples. 500 mg of NH_2-MIL-53(Al) powers were placed in a silica boat, which carbonized at 700, 800, 900 and 1000 °C in a tube furnace. The temperature was elevated to corresponding carbonized temperature with a heating speed of 5 °C·min^{-1} and maintained for 3 h under Argon atmosphere with a gas flow of 70 mL·min^{-1}. Then, all those products were immersed in hydrochloric acid (1M, 10 mL) for 1 hour. After centrifugation, the NPC-MIL-700, NPC-MIL-800, NPC-MIL-900, and NPC-MIL-1000 products were obtained at 700, 800, 900, 1000 °C.

2.4 Materials Characterization

The morphologies of the power were obtained by Scanning electron microscopy (SEM) images on Nova NanoSEM 450. Transmission electron microscope (TEM) images were taken by Tecnai G2 F20. The Powder X-ray diffraction (XRD) patterns were obtained by using a D-MAX 2500/PC with a graphite-monochromated Cu Kα radiation source. X-ray photoelectron spectroscopy (XPS) was obtained by using a ThermoFisher ESCALAB 250xi. Raman spectrum was measured on a LabRAM HR-800 Raman spectrometer. The nitrogen adsorption and desorption isotherms measurement were carried out by AutoChemi II2920 at 77 K.

2.5 Electrochemical measurements

A conventional three-electrode was used for electrochemical measurements by using VSP-300 electrochemical workstation (Bio-Logic SAS, France) at 25 °C. 0.3 mL alcohol, 0.3 mL deionized water,

0.05 mL Nafion solution (5wt%) and 5 mg NPC-MIL-n or Pt/C catalysts were adequately mixed together by ultrasonic machine. Then, 8 μL of the mixture was dropped onto the clear glassy carbon disk electrode (diameter = 0.4 cm), which was used as a working electrode. A platinum wire and an Ag/AgCl were utilized as a counter electrode and a reference electrode, respectively. During the measurement, O_2-saturated 0.1 M KOH aqueous solution was used as the electrolyte.

Cyclic voltammetry (CV) was scanned at a rate of 50 mV s^{-1} in the potential range from 0 to −0.8 V. The rotating disk electrode (RDE) measurement was used with the speed from 400 to 2025 rpm at a scanning rate of 5 mV s^{-1}. The rotating ring-disk electrode (RRDE) measurement was used at a rotating speed of 1600 rpm at a scanning rate of 5 mV s^{-1} in O_2-saturated 0.1 M KOH aqueous solution.

3. RESULTS AND DISCUSSION

3.1 Physical characterization of NPC-MILs

First, NH_2-MIL-53(Al) was prepared by the hydrothermal reaction according to previous literature,[26] which was chosen as a precursor for ORR electrocatalyst. Then, NH_2-MIL-53(Al) was transformed into the NPC-MILs via carbonization and acidation. In addition, the NPC-MILs have better conductivity than carbon materials, which is conducive to the electron transfer during electrocatalysis such as ORR.[27-29] The synthesis of NH_2-MIL-53(Al) crystals were prepared for the volume ratio of water and DMF (1:0.5, 1:1, 1:2, 1:3, 1:4). After pyrolyzing, only those of 1:1, 1:3, 1:4 can be successfully carbonized and the linear sweep voltammograms (LSV) curves of corresponding materials are shown in Fig. S1. It can be found when the volume fraction of water and DMF is 1:1, the material has highest electrocatalytic activities. So the volume ratio of 1:1 was chosen to synthesize precursor in this work. Then, to explore the influence of annealing temperature, we investigated electrocatalytic activities of carbonized temperature from 700 to 1000 ^oC. The LSV curves are presents in Fig. S2. From the figure, it can be found that P-NPC-MIL-900 shows the best onset potentials and the highest current densities of the four catalysts. Therefore, 900 ^oC was selected as annealing temperature. Meanwhile, acidification is another important method to improve electrocatalytic activities. This method can remove the template of raw materials and some unreacted impurities. The LSV curves of NH_2-MIL-53(Al), P-NPC-MIL-900 (unacidified material) and NPC-MIL-900 are shown in Fig. S3. It can be found that NPC-MIL-900 has better electrocatalytic activities than the others. So, in this work, the NPC-MIL-900 was be synthesized after carbonization and acidification of NH_2-MIL-53(Al). The ICP-MS analysis validated the absence of traceable Al species in the NPC-MIL-900.

The morphology of the NH_2-MIL-53(Al) and NPC-MIL-900 were investigated using scanning electron microscopy (SEM) and transmission electron microscopy (TEM) (as shown in Fig. 1). It is obvious to see that the NH_2-MIL-53(Al) has uniform diameter of ~50 nm, length of ~200 nm (Fig. 1a and 1c), and the shape is a cylinder with the end of the round. In Fig. 1b and 1d, the images clearly show that after carbonization, the skeleton of NPC-MIL-900 is well remained, while the microstructures were obviously shrunken accompanied with the appearance of more pores on the surface. This is to say, high temperature prompted the NPC-MIL-900 surface with more porous and rough, but the original skeleton

and structure of MOFs were inherited. The textural property and inner structure of NPC-MIL-900 can be further investigated by N_2 sorption isotherms and pore size distribution analysis in Fig. 2a. According to the IUPAC classification, NPC-MIL-900 demonstrated a type-IV curve with a type-H3 hysteresis,[30] which is confirming the existence of mesoporous. The synthesized NPC-MIL-900s BET surface area is 348 m^2/g with uniform pore size about 3.9 nm (Fig. 2a), which allow exposure of competent active sites and facilitates O_2 and electrolyte transport in the ORR performance.[31]

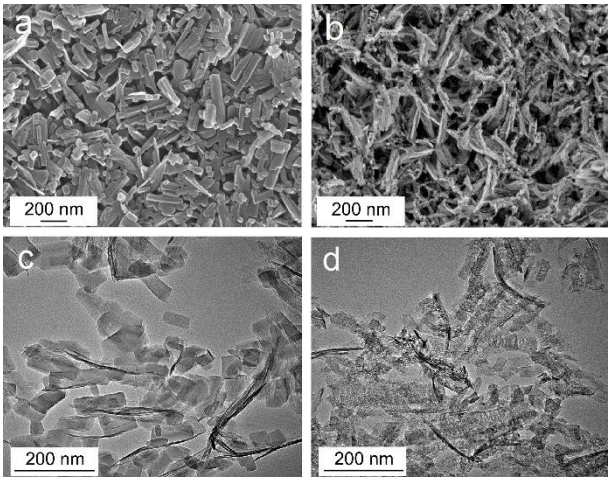

Figure 1. SEM (a, b) and TEM images (c, d) of NH_2-MIL-53(Al) (a, c) and NPC-MIL-900 (b, d).

The composition of the NPC-MIL-900 was also analyzed by different characterization techniques including X-ray diffraction (XRD) survey, Raman spectroscopy and X-ray photoelectron spectroscopy (XPS). In the XRD pattern of NPC-MIL-900 (Fig. 2b), the characteristic diffraction peaks at $2\theta = 44°$ may be assigned to (101) planes of graphitic carbon. For the detailed structural information of graphitic carbon in the NPC-MIL-900 was also evaluated by Raman spectrum in Fig. 3a. As can be seen in the figure, two typical Raman peaks of carbon can be observed. The peak at 1320-1330 cm^{-1} can be assigned to the D-band peak and that at 1590 cm^{-1} is assigned to the G band, which related to the defects and disorder degree of carbon and order degree of graphitization, respectively. The high ratio of I_D/I_G (I_D/I_G = 0.93) and the board peaks indicate that carbon of the NPC-MIL-900 is highly disordered.[32]

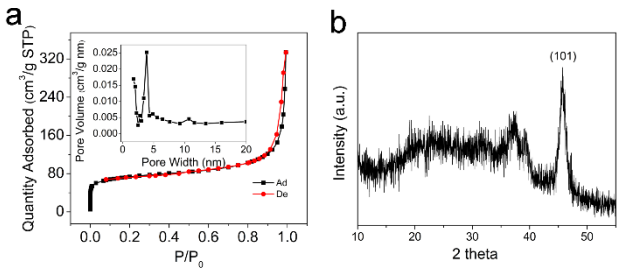

Figure 2. (a) N_2 adsorption-desorption isotherm of NPC-MIL-900, and the corresponding pore size distribution is shown in inset; (b) XRD pattern of NPC-MIL-900.

The composition was further studied by XPS measurement in Fig. 3b, 3c, 3d. The survey XPS spectrum (Fig. 3b) showed the existence of C, O and N, which indicate the successful synthesis of nitrogen-doped carbonization. The C1s XPS spectrum in Fig. 3c presents several characteristic peaks, where the peaks at 284.8 and 285.5 eV correspond to the C=C and the C−C, the peaks at 286.9 and 288.5 eV are assigned to C=O and C−N, respectively. N1s binding energy spectrum of the NPC-MIL-900 is shown in Fig. 3d. The figure present three kinds of N1s peaks at 398.53, 400.15 and 401.02 eV, corresponding to pyridinic, pyrrolic and graphitic N, respectively.[33] N-doped carbonization can enhance the degree of defectiveness, which enhance the active sites and promote the ORR activity. Particularly, graphitic and pyridinic-N groups can offer more active sites than pyrrolic counterpart.[34]

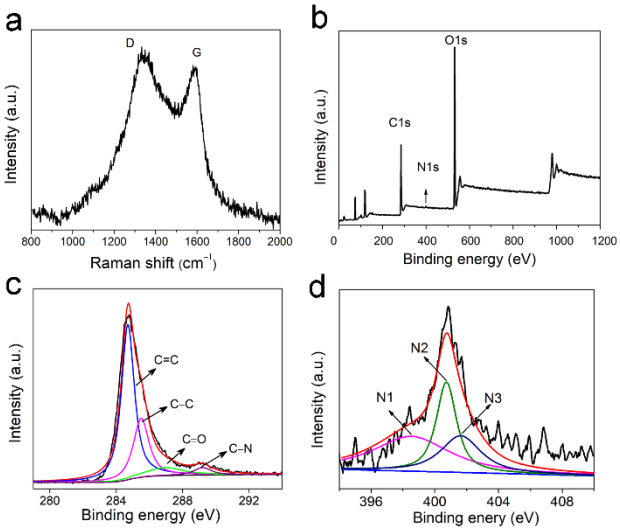

Figure 3. (a) Raman spectrum of NPC-MIL-900; (b, c, d) XPS spectra of NPC-MIL-900; (b) survey spectrum, (c) C1s binding energy spectrum, and (d) N1s binding energy spectrum.

3.2 Oxygen Reduction Reaction of NPC-MILn

To gain insight into structure-activity relationship, the ORR electrocatalytic activities of the NPC-MIL-900 catalysts were first evaluatedin O_2 saturated 0.1 M KOH aqueous solution by cyclic voltammetry (CV) at 25 ºC in Fig. 4a. As can be seen in the figure, a well-defined O_2 reduction peak centered at 0.76 V (vs RHE) emerges. The LSVs curves of the commercial Pt/C (20 wt%), NH_2-MIL-53(Al) and NPC-MIL-900 are shown in Fig. 4b. The onset potential of NPC-MIL-900 at 0.82 V trends towards commercial Pt/C （0.96 V） and the half-wave potential of NPC-MIL-900 at 0.76 V trends commercial Pt/C (0.85 V). The diffusion-limited current density of NH_2-MIL-53(Al), NPC-MIL-900 and Pt/C are 1.3, 4.9, 6.1 mA/cm^2, respectively. It means after carbonization, the electrochemical ORR activity of NPC-MIL-900 significantly enhanced and close to Pt/C electrodes. It can be explained that the more pore and larger surface area enhance the ORR activity on account of boost the mass transport. More porous carbon-based catalysts comparisons are shown in Table 1. Furthermore, to state the ORR kinetic performance involving the NPC-MIL-900 catalysts, the LSV curves on RDE were recorded over a range of electrode rotation speeds from 400 to 2025 rpm in Fig. 4c. It can be found with the increase

of rotation speed, the diffusion-limited current density increased. The corresponding Koutecky-Levich (K-L) plots are shown in Fig. 4d and the linear plots indicate the first order reaction kinetics toward oxygen.[35] Based on the K-L equations, the electron transfer number (*n*) of NPC-MIL-900 was 3.3 over the potential range from 0.3 to 0.7 V. In order to further explain the electrocatalytic performance and the better investigation of the mass transfer kinetics of NPC-MIL-900 and Pt/C, a RRDE measurement was also measured at the same condition in Fig. S4. The electron transfer number (*n*) of NPC-MIL-900 was calculated to be 3.6. These results show that a likeness four-electron process is the state pathway for the oxygen reduction at NPC-MIL-900 electrode.[36]

Table 1. Comparison of the electrocatalytic performance of porous carbon-based catalysts reported.

Comparison of the electrocatalytic performance of porous carbon-based catalysts reported			
Catalyst	Onset potential(V *vs.* RHE)	Electron transfer number	Ref
N-doped C	1.135	3.9@ 0.5 V	37
NPS-C-MOF-5	~0.9	3.6@ 0.42 V	38
3D-TDGC-900	0.97	3.97@ 0.5 V	39
MPSA/GO/1000	~0.93	3.7@ 0.65 V	40
GZxC	0.88	3.2 @ 0.6 V	41
NPGC-950	0.91	3.79@ 0.1-0.4 V	42
PBDTTT-C-T	0.93	~4.0@ 0.4-0.7 V	43
HPCF-800	0.88	4.0 @0.6 V	44
FS350Z-900	1.00	3.3@ 0.3-0.5 V	45
PDMC-800	0.94	3.78@ 0.5 V	46

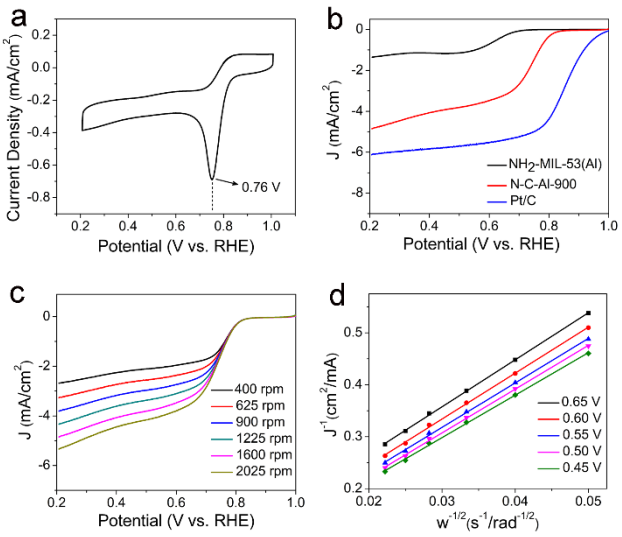

Figure 4. (a) CV curve of NPC-MIL-900 in O_2-saturated solution at a scan rate of 50 mV/s; (b) LSV curves of NH_2-MIL-53(Al), NPC-MIL-900 and Pt/C at a rotation rate of 1600 rpm; (c) LSV curves of NPC-MIL-900 in O_2-saturated solution with 0.1 M KOH of various rotation rate; (d) K-L plots of NPC-MIL-900 derived from LSV cures at different electrode potentials.

Stability is quite important for catalysts in fuel cell technology. The stability of NPC-MIL-900 was measured by the chronoamperometric measurement at −0.6 V (vs. RHE) in O_2-saturated 0.1 M KOH electrolyte at a rotating speed of 1600 rpm. As a comparison, Pt/C (20 wt%) was also measured under the identical experimental condition (Fig. 5a). It can be found that the current density of the NPC-MIL-900 shows less decay than that of the commercial Pt/C. After 40000 s, about 13% loss at the current density is occurred at NPC-MIL-900 catalyst, whereas the corresponding current loss at the Pt/C is as high as 31%. It demonstrates that the NPC-MIL-900 has a better stability than Pt/C catalyst for the ORR. The methanol poisoning effect is another issue that needs to be settled in the direct methanol fuel cells (DMFCs). Chronoamperometric responses of NPC-MIL-900 and Pt/C electrodes were investigated at −0.6 V (vs. RHE) in O_2-saturated 0.1 M KOH electrolyte at a rotating speed of 1600 rpm for 1300 s in Fig. 5b. After injecting 1 M methanol at 300 s, the voltammetric current of NPC-MIL-900 catalyst decreases and the current maintains about 96% in the same process, which is higher than that of Pt/C. These results indicate that the NPC-MIL-900 catalyst can not only keep high stability but also perform high methanol tolerance in ORR.

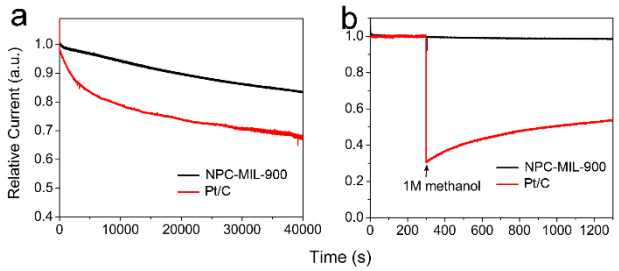

Figure 5. (a) Current-time (i-t) chronoamperometric responses at −0.6 V (vs. RHE) in O_2-saturated 0.1 M KOH at NPC-MIL-900 and Pt/C electrodes (1600 rpm) for 40000 s; (b) Chronoamperometric responses at −0.6 V in O_2-saturated 0.1 M KOH at NPC-MIL-900 or Pt/C electrodes (1600 rpm) before and after injection of 1 M methanol.

4. CONCLUSIONS

In summary, NPC-MILs have been synthesized by direct carbonization and acidification of an amine functionalized Al-MOFs (NH_2-MIL-53(Al). The physical structure character and the electrocatalytic performance were fully investigated by various characterization methods. The NPC-MIL-900 (carbonized at 900 °C) as metal-free electrocatalysts are demonstrated promising potential for ORR. It shows good ORR activity comparable to commercial Pt/C and exhibits a likeness four-electron process. What's more, the as-prepared NPC-MIL-900 catalyst not only shows better stability but also performs higher methanol tolerance than the Pt/C catalysts toward ORR in the alkaline system. This work provides a simple and scalable route for preparing N-doped-porous-carbon material with great prospects in energy applications. As a metal-free electrocatalyst, N-doped atoms and porosity may promote the performance of the porous carbon product for ORR, which is an crucial factor of the performance of a fuel cell.

ACKNOWLEDGEMENT
This work was supported by the Natural Science Foundation of China (Grant Nos. 21475071, 21703115), the Natural Science Foundation of Shandong Province (Project No. ZR2016BQ44, 2018GGX102030), the Taishan Scholar Program of Shandong Province (ts201511027)

CONFLICT OF INTEREST
The authors declare no conflict of interest.

SUPPORTING INFORMATION

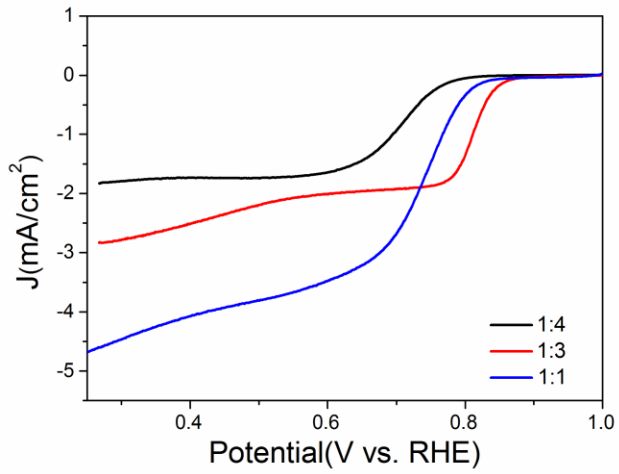

Fig. S1. LSV cures of three volume ratio of water and DMF (1:1, 1:3, 1:4) at a rotation rate of 1600 rpm.

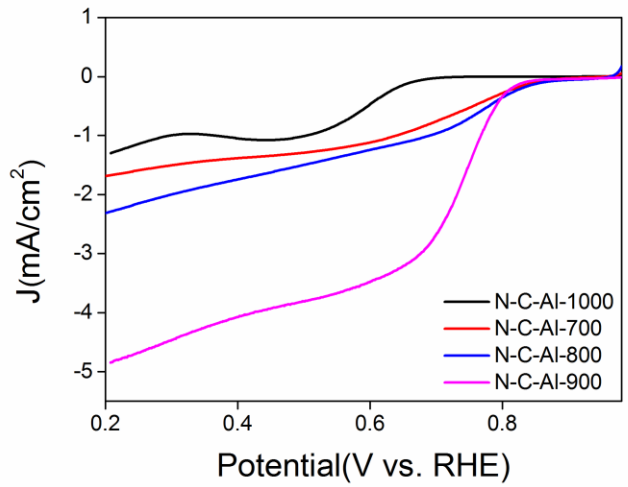

Fig. S2. LSV cures of N-C-Al-700, N-C-Al-800, N-C-Al-900 and N-C-Al-1000 at a rotation rate of 1600 rpm.

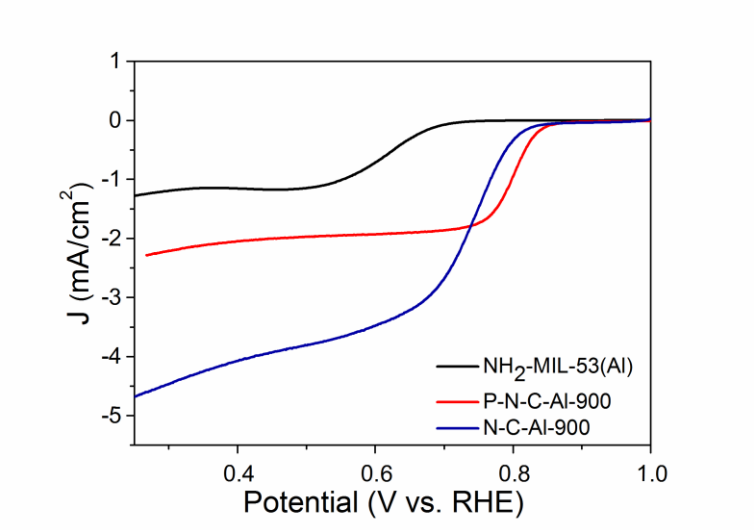

Fig. S3. LSV cures of NH_2-MIL-53(Al), P-N-C-Al-900 and N-C-Al-900 and at a rotation rate of 1600 rpm.

References

1. M. Winter, R. J. Brodd, *Chem. Rev.*, 104(2004)4245.
2. M. A. Hannan, M. S. H. Lipu, A. Hussain, A. Mohamed, Renew., *Sust. Energ. Rev.*, 78(2017)834.
3. S. Y. Wang, S. P. Jiang, *Natl. Sci. Rev*, 4(2017)163.
4. M. H. Shao, Q. W. Chang, J. P. Dodelet, R. Chenitz, *Chem. Rev.*, 116(2016)3594.
5. D. H. Guo, R. Shibuya, C. Akiba, S. Saji, T. Kondo, J. Nakamura, *Science*, 351(2016)361.
6. J. Park, Y. Nabae, T. Hayakawa, M.-a. Kakimoto, *ACS Catal.*, 4(2014)3749.
7. W. J. Jiang, L. Gu, L. Li, Y. Zhang, X. Zhang, L. J. Zhang, J. Q. Wang, J. S. Hu, Z. Wei, L. J. Wan, *J. Am. Chem. Soc.*, 138(2016)3570.
8. K. Miyabayashi, M. Miyake, *Chem. lett.*, 46(2017)707.
9. H. M. Barkholtz, D. J. Liu, *Mater. Horizons*, 4(2017)20.
10. J. Kim, Y. Lee, S. Sun, *J. Am. Chem. Soc.*, 132(2010)4996.
11. L. Yao, W. H. Zhong, L. Qiu, L. B. Deng, *Int. J. Electrochem. Sci*., 13(2018)5798.
12. S.R. Batten, N.R. Champness, X.-M. Chen, J. Garcia-Martinez, S. Kitagawa, L. Öhrström, M. O'Keeffe, M.P. Suh, J. Reedijk, *Pure Appl. Chem.*, 85(2013)1715.
13. Y. F. Yang, R. Sakashita, K. Yamasumi, M, Ishida, T. Yamada, H, Furuta, *Chem. lett.*, 46(2017)1230.
14. A. Morozan, M. T. Sougrati, V. Goellner, D. Jones, L. Stievano, F. Jaouen, *Electrochim. Acta*, 119(2014)192.
15. Y. J. Sa, D. J. Seo, J. Woo, J. T. Lim, J. Y. Cheon, S. Y. Yang, J. M. Lee, D. Kang, T. J. Shin, H. S. Shin, *J. Am. Chem. Soc.*, 138(2016)15046.
16. J. Li, S. Ghoshal, W. Liang, M.-T. Sougrati, F. Jaouen, B. Halevi, S. McKinney, G. McCool, C. Ma, X. Yuan, Z.-F. Ma, S. Mukerjee, Q. Jia, *Energy Environ. Sci*., 9(2016)2418.
17. K. Artyushkova, A. Serov, S. Rojas-Carbonell, P. Atanassov, *J. Phys. Chem. C*, 119(2015)25917.
18. Q. Jia, N. Ramaswamy, U. Tylus, K. Strickland, J. Li, A. Serov, K. Artyushkova, P. Atanassov, J. Anibal, C. Gumeci, S.C. Barton, M.-T. Sougrati, F. Jaouen, B. Halevi, S. Mukerjee, *Nano Energy*, 29(2016)65.

19. F. Yusoff, N. Mohamed, A. Azizan, S. A. Ghani, *Int. J. Electrochem. Sci*., 11(2016)5766.
20. K. Elumeeva, J. Ren, M. Antonietti, T.-P. Fellinger, *ChemElectroChem.*, 2(2015)584.
21. Q. X. Lai, J. J. Zhu, Y. X. Zhao, Y. Y. Liang, J. P. He, J. H. Chen, *Small*, 13(2017)1700740.
22. S. L. Zhao, Y. Wang, J. C. Dong, C. T. He, H. J. Yin, P. F. An, K. Zhao, X. F. Zhang, S. Q. Liu, H. J. Zhao, Z. Y. Tang, *Nat. Energy*, 1(2016)1.
23. H. R. Ong, C. W. Woon, M. S. Ahmad, A. Yousuf, C. K. Cheng, M. M. R. Khan, *Int. J. Electrochem. Sci*., 13(2018)7789.
24. X. Gu, Y. Wang, L. T. Yan, L. J. Li, P. C. Dai, H. B. Wang, X. B. Zhao, *Int. J. Electrochem. Sci*., 11(2016)9575.
25. A. Aijaz, N. Fujiwara, Q. Xu, *J. Am. Chem. Soc.*, 136(2014)6790.
26. X. Q. Cheng, A. F. Zhang, K. K. Hou, M. Liu, Y. X. Wang, C. S. Song, G. L. Zhang, X. W. Guo, *Dalton Trans*., 42(2013)13698.
27. S. W. Liu, M. Y. Tong, G. Q. Liu, X. Zhang, Z. M. Wang, G. Z. Wang. H. P. Cai, H. M. Zhang, H. J. Zhao, *Inorg. Chem. Front*, 4(2017)491.
28. S. L. Zhao, H. J. Yin, L. Du, L. C. He, K. Zhao, L. Chang, G. P. Yin, H. J. Zhao, S. Q. Liu, Z. Y. Tang, *Acs Nano*, 8(2014)12660.
29. Y. Q. Wang, L. Tao, Z. H. Xiao, R. Chen, Z. Q. Jiang, S. Y. Wang, *Adv. Funct. Mater*., 28(2018)1705356.
30. F. Afsahi, S. Kaliaguine, *J. Mater. Chem. A*, 2(2014)12270.
31. Y. Liu, X. F. Zeng, W. C. Wang, D. P. Cao, *Adv. Funct. Mater*., 28(2018)1704537.
32. Y. Hou , T. Z. Huang, Z. H. Wen, S. Mao, S. M. Cui, J. H. Chen, *Adv. Energy Mater*., 4(2014)140037.
33. P. H. Matter, L. Zhang, U. S. Ozkan, *J. Catal*., 239(2006)83.
34. L. Li, P. Dai, X. Gu, Y. Wang, L. Yan, X. Zhao, *J. Mater. Chem. A*, 5(2017)789.
35. H. Y. Zhu, S. Zhang, Y. X. Huang, L. H. Wu, S. H. Sun, *Nano Lett*., 13(2013)2947.
36. E. A. Franceschini, M. M. Bruno, F. A. Viva, F. J. Williams, M. Jobbágy, H. R. Corti, *Electrochim. Acta*, 71(2012)173.
37. S. Gao, K. Geng, H. Liu, X. Wei, M. Zhang, P. Wang, J. Wang, *Energy Environ. Sci.*, 8(2015)173.
38. J. S. Li, S. L. Li, Y. J. Tang, K. Li, L. Zhou, N. Kong, Y. Q. Lan, J. C. Bao, Z. H. Dai, *Sci. Rep.*, 4(2014)1.
39. M. S. A. S. Shah, J. Lee, A. Rauf, J. H. Park, B. Lim, P. J. Yoo, *Nanoscale*, 10(2018)19498.
40. J. Zhang, L. Qu, G. Shi, J. Liu, J. Chen, L. Dai, *Angew. Chem., Int. Ed.*, 55(2016)2230.
41. M. Thomas, R. Illathvalappil, S. Kurungot, B. N. Nair, A. A. Mohamed,G. M. Anilkumar, T. Yamaguchi, U. S. Hareesh, *ACS Appl. Mater. Interfaces.*, 8(2016)29373.
42. M. Bao, Y. Sun, M. Li, C. Hu, Z. Man, L. Wang, T. Yang, Y. Chen, P. Wan, J. Pan, *ACS Appl. Mater. Interfaces*, 8(2016)1415.
43. L. Zhang, X. Wang, R. Wang, M. Hong, *Chem. Mater.*, 27(2015)165.
44. Z. Guo, C. Jiang, C. Teng, G. Ren, Y. Zhu, L. Jiang, *ACS Appl. Mater. Interfaces*, 6(2014)21454.
45. C. Guo, R. Hu, W. Liao, Z. Li, L. Sun, D. Shi, Y. Li, C. Chen, *Electrochim. Acta*, 236(2017)228.
46. R. Silva, D. Voiry, M. Chhowalla, T. Asefa, *J. Am. Chem. Soc.*, 135(2013)7823.